# CHAPTER IV
RESULTS AND DISCUSSION

4.1 The Chemical and Physical Structure of Polybenzoxazine Precursors

Organic xerogel processing normally use phenol compounds and formaldehyde as precursors. As observed from many studies, there are many synthesis parameters affecting properties of the resulting xerogel, such as concentration of precursor solution, type of solvent, phenol to formaldehyde ratio, additive content, catalyst content, rate of carbonization and gelation time (Qin and Guo, 2001; Wu and Fu, 2005). Organic xerogels can derived from various organic precursors. However, in all recent type of precursors, 4,4-Diaminodiphenylmethane is the novel type of amine.
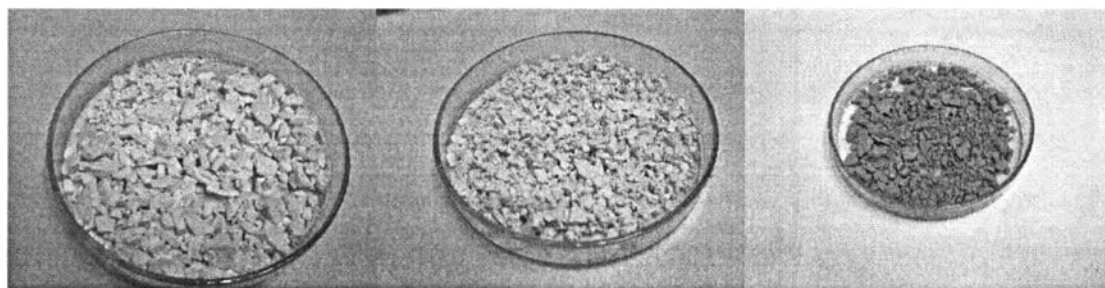
(a) Polvbenzoxazine (b) Polybenzoxazine after drying (c) Polybenzoxazine after curing

Figure 4.1 shown pictures of Polybenzoxazine (a) polybenzoxazine, (b) polybenzoxazine after drying (c) polybenzoxazine after curing.

The chemical structure of benzoxazine precursor was examined by FTIR spectra as shown in Figure 4.2 The characteristic absorption bands at 1230-1234 cm^{-1} (asymmetric stretching of C-O-C of oxazine), 922 cm^{-1} (out-of-plane bending vibrations of C-H) and 1500 cm^{-1} (trisubstituted benzene ring) were observed (Figure 4.2(a,b)).

Additionally, the characteristic absorption assigned to the stretching of trisubstituted benzene ring at 1500 cm^{-1} and the out-of-plane bending vibrations of C-H at 922 cm^{-1} were detected, indicating the presence of the cyclic benzoxazine structure in the backbone of the precursor. After polymerization at 165 °C, the intensity of trisubstituted benzene ring at 1500 cm^{-1} of the fully cured polybenzoxazine xerogels,

almost disappeared. This indicated that the resulting organic aerogel could be completely cured by using this proposed step curing method. Due to the similar appearance of the fully cured polybenzoxazine and fully cured polybenzoxazine xerogel absorption bands, it could be inferred that after the ambient drying and curing process, there was no detectable amount of dimethylformamide remaining in the resulting aerogel, although the drying period was only a couple of days.

Moreover, the spectrum could confirm that a chemical interaction between the polybenzoxazine and the dimethylformamide did not exist during this process. From the spectra of fully cured polybenzoxazine xerogels (Figure 4.2c), the obvious changes in absorbance due to chemical transformations from the polybenzoxazine organic xerogel to carbon xerogel could be easily observed.

After the organic xerogels were carbonized at 800 °C, the characteristic absorption bands of the organic compound were no longer seen. This result strongly agrees with the study of Li *et al.* which investigated the chemical and physical changes during the pyrolysis process of cresol–formaldehyde. They observed that the intensity of the organic absorption peaks becomes weaker with an increase of pyrolysis temperature, and the absorption peaks almost completely disappear at 800 °C. They also suggested that the aromatic rings rearrange themselves, leading to bound carbon rings during the pyrolysis.
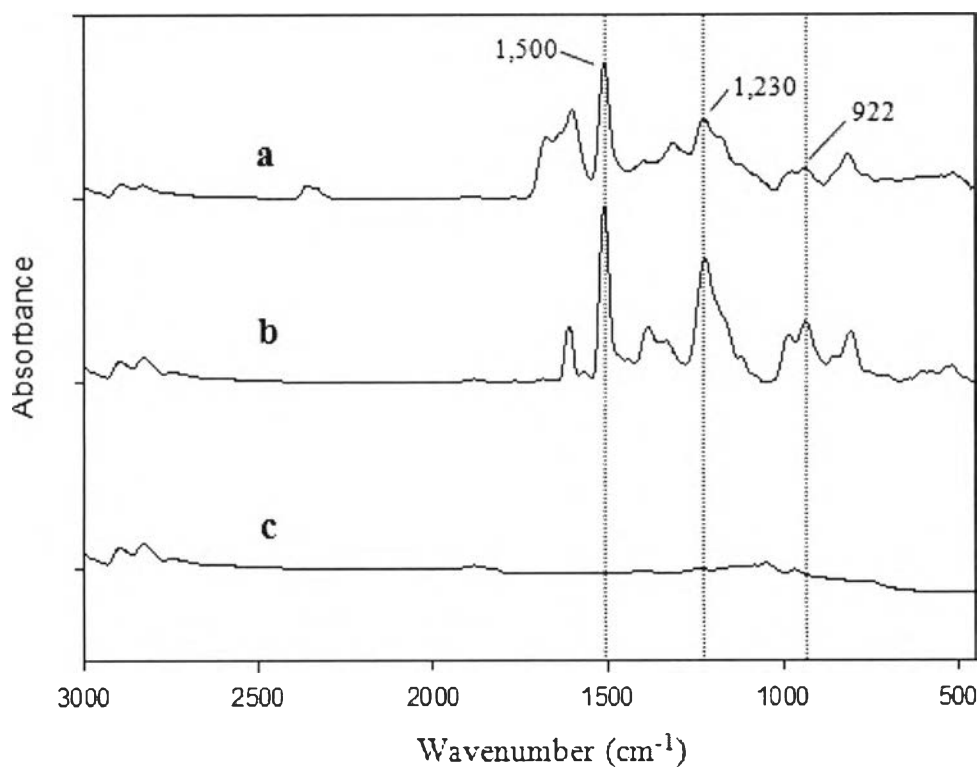
Figure 4.2 FTIR spectra of 25% w/w of benzoxazine precursor added with Poly (ethylene glycol)-*block*-poly(propylene glycol)-*block*-poly(ethylene glycol) 0.09M using different step (a) fully cured polybenzoxazine, (b) uncured polybenzoxazine, and (c) carbon xerogel.

4.2 Thermal Behaviors of Polybenzoxazine Precursors

The investigation of the static curing temperature of the benzoxazine resin was accomplished by using DSC with a relatively slow heating rate of 1°C/min. Figure 4.3 shows the DSC thermogram of curing exothermic peak of the benzoxazine monomer. As seen from this figure, the exothermic peak of the monomer, corresponding to its ring opening polymerization, was located at 120 – 240 °C. In order to clarify the appropriate curing temperature, both the curing temperature of the resin and the boiling temperature of the solvent have to be considered. Based on the DSC result, a curing temperature of 165°C was used in this study because it can produce the polymerization reaction of benzoxazine without boiling the dimethylformamide (153°C) because the solvent was removed from the benzoxazine after exchange solvent by acetone and drying in the oven. Figure 4.3 (a) shows the exothermic peak from 160-170 °C of benzoxazine precursor while the exothermic peak of polybenzoxazine disappeared as shown in Figure 4.3 (b). These obviously show that the polymerization of benzoxazine precursor by ring-opening of oxazine was taken place.
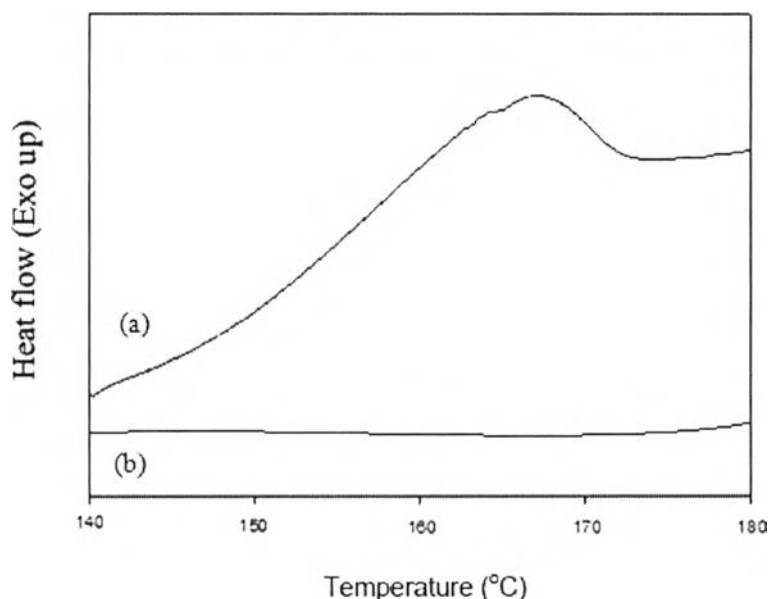
Figure 4.3 DSC thermograms of (a) the polybenzoxazine precursor after drying at 80°C (pre-cured) for 2 days and (b) after heat treatment at 180 °C (fully-cured).

The TGA thermogram of the fully-polymerized polybenzoxazine shown in Figure 4.4 It began to lose weight at 300°C, and high mass loss rate was observed in the temperature range of 300 – 600 °C, which was caused by the production of a large amount of volatile materials. The rate of mass loss became smaller after 600 °C. According to this TGA thermogram, the carbon xerogels were prepared by the pyrolysis of organic xerogels following the three ramp cycles from: 30°C to 300°C, 300°C to 600°C, and 600 to 800°C. Moreover, it can be seen that the char yield at 800°C was 23 wt%. Kasinee *et al.* (2002) identified the decomposition products of aromatic amine-based polybenzoxazines through TGA and GC-MS techniques. They found that the decomposition products were a combination of benzene derivatives, amines and phenolic compounds. In contrast, the thermal decomposition temperature was enhanced for the PBZ xerogel added with Poly(ethylene glycol)-*block*-poly(propylene glycol)-*block*-poly(ethylene glycol) 0.09M and the char yield of the PBZ xerogel added with Poly(ethylene glycol)-*block*-poly(propylene glycol)-*block*-poly(ethylene glycol) 0.09M was significantly increased.
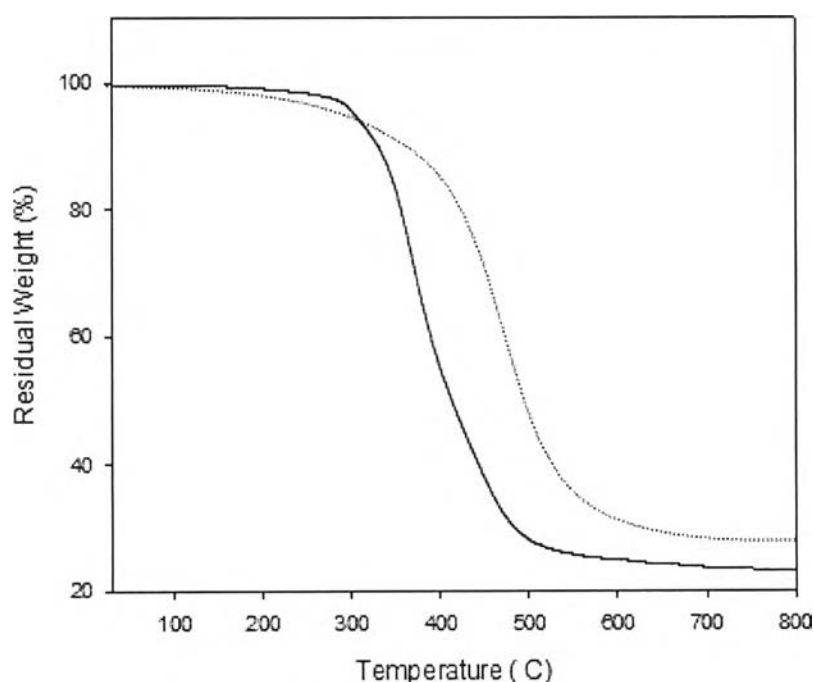
Figure 4.4 TGA thermogram of PBZ xerogels (⎯⎯) and PBZ xerogels added with Poly(ethylene glycol)-*block*-poly(propylene glycol)-*block*-poly(ethylene glycol) 0.09M (⸳⸳⸳⸳⸳).

4.3 The density and porosity of material from gaspycnometer.

Finding the surface area to calculate the porosity of carbon xerogel has almost done by BET method, But for aromatic amine structure which has very dense organic xerogel cannot turn to carbon xerogel and porosity and density of the organic xerogel was characterized using helium pycnometry. This method provides skeletal volume, density and porosity of the determined material. (Parmentier *et al.*, 2001)

Density, also an important physical property of the xerogel material, was measured by ultrapycnometer gas meter.

$$Density = \frac{Weight\ of\ material}{Volume\ of\ material}$$

The densities of MDA (aromatic amine) and TETA (aliphatic amine) were compared shown in Table 4.1. The density of the MDA organic xerogel was lower than TETA because aromatic ring structure lead to the fuse of carbon xerogel of MDA while carbonization in Figure 4.5.
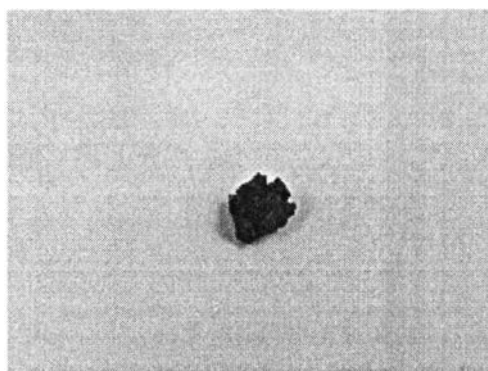
Figure 4.5 Fuse carbon xerogel of 4,4-Diaminodiphenylmethane.

$$\frac{1}{\rho} - \frac{1}{\rho s} = porosity$$

ρ = bulk density

ρ_s = skeleton density

The bulk volume was measured by Vernier Caliper and the average volume was measured by ultrapycnometer gas meter, and then calculated % porosity from

above equation. When compare MDA (aromatic amine) with TETA (aliphatic amine), the porosities of MDA and TETA were about 62% and 74%, respectively as shown in Table 4.1.

From this studied, aromatic amine cannot change from organic xerogel to be carbon xerogel because the aromatic structure as obviously shown by density and %porosity in the table below. In MDA, the volatile chemical or solvent cannot go out from the porous structure lead to fusion of porous material.

Table 4.1 shown average density and % porosity of various amine

Sample	MDA (Aromatic amine)	TETA (Aliphatic amine)
Avg Density (g/cc)	0.86	0.74
% porosity	62%	74%

4.4 Effects of Nonionic surfactant (Poly(ethylene glycol)-*block*-poly(propylene glycol)-*block*-poly(ethylene glycol)) on porous structure of PBZ-based organic xerogels

Polybenzoxazine (PBZ)-based carbon xerogels were synthesized by using Poly(ethylene glycol)-*block*-poly(propylene glycol)-*block*-poly(ethylene glycol) as a non-ionic surfactant as described in experimental section. The morphologies of the obtained PBZ-based carbon xerogels were observed by FE-SEM technique. Figure 4.6 shows the SEM micrographs of PBZ-based organic xerogels synthesize by adding Poly(ethylene glycol)-*block*-poly(propylene glycol)-*block*-poly(ethylene glycol) was shown the inter-connected network formed.
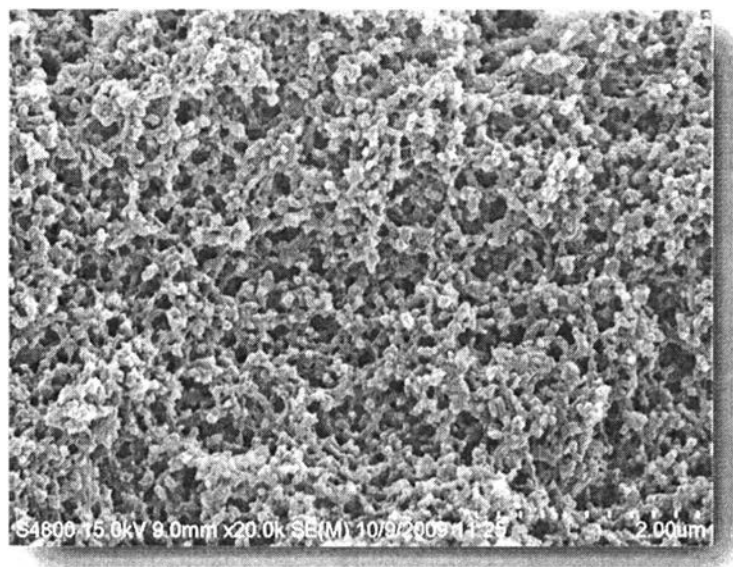
Figure 4.6 SEM micrograph of the carbon xerogel derived from 25 wt% of polybenzoxazine with Poly(ethylene glycol)-*block*-poly(propylene glycol)-*block*-poly(ethylene glycol).

To explain the formation of carbon xerogel microspheres, the micelle formation of Poly(ethylene glycol)-*block*-poly(propylene glycol)-*block*-poly(ethylene glycol) can explain by Figure 4.7. If the concentration of poly(ethylene glycol)-*block*-poly(propylene glycol)-*block*-poly(ethylene glycol) was equal the critical micelle concentration (CMC), the molecules of poly(ethylene glycol)-*block*-poly(propylene glycol)-*block*-poly(ethylene glycol) was then oriented as spherical shape with hydrophilic head group at exterior region and hydrophobic tail group at interior region of the micelle. Polybenzoxazine cluster will be then formed at the interior region of the micelle and then growth into microspherical shape. After that, the interconnection between benzoxazine microspheres can be taken place due to the ring opening polymerization of oxazine ring at the surface of each microsphere. As illustrated in figure 4.7 is the formation model of polybenzoxazine xerogel microspheres formed inside the interior region of Poly(ethylene glycol)-*block*-poly(propylene glycol)-*block*-poly(ethylene glycol) micelle. In 2011, Wang *et al.* found that carbon aerogel microspheres could be produced by using non-ionic surfactant, called SPAN 80, in the range of 2-50 μ m in sizes.

Microsphere of Poly(ethylene glycol)-*block*-poly(propylene glycol)-*block*-poly(ethylene glycol) system

Benzoxazine-Micelle system
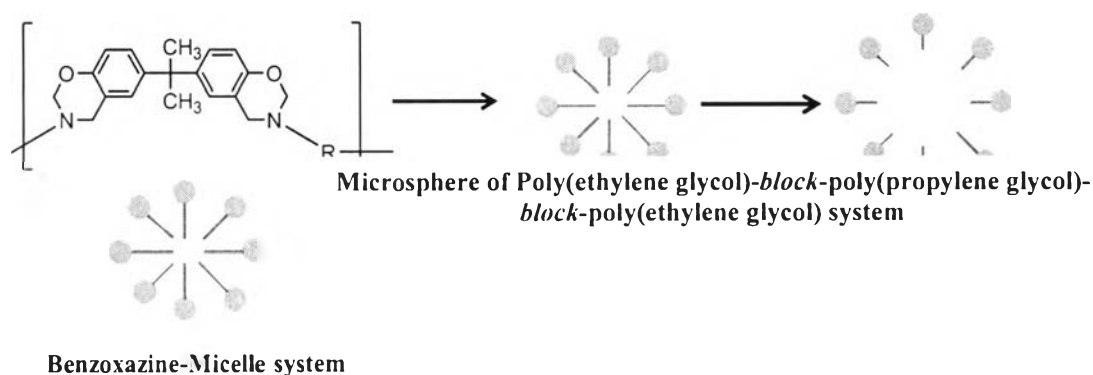
Figure 4.7 Formation model of microsphere of Poly(ethylene glycol)-block-poly(propylene glycol)-block-poly(ethylene glycol) system.

The porous structures of PBZ-based organic xerogels using Poly(ethylene glycol)-*block*-poly(propylene glycol)-*block*-poly(ethylene glycol) as a surfactant were tabulated in Table 4.2. All samples show the comparative BET surface area about 9-15 m^2/g. Higher amount of mesopore volume comparing to micropore volume was obtained about 0.10 cc/g for OX-Surfactant-0.030. However, when the concentration of Poly(ethylene glycol)-*block*-poly(propylene glycol)-*block*-poly(ethylene glycol) was changed from 0.009 M to 0.090 M, the samples showed constant amount of micropore volume about 0.01 cc/g and 0 cc/g at concentration 0.090 M. Pointing to an average mesopore diameter of all samples, we found that an average mesopore diameter was increased from 3.59 nm to 4.58 nm. The expansion of mesopore diameter from 3.59 nm for OX-Surfactant-0.003 to 4.58 nm for OX-Surfactant-0.009 could be explained by the enlargement of Poly(ethylene glycol)-*block*-poly(propylene glycol)-*block*-poly(ethylene glycol) benzoxazine chain spacing resulted from the molecules.

According to the IUPAC classification, it was found that the adsorption isotherms of all samples are a standard isotherm between type IIb isotherm in which type IIb represents macroporous adsorbent. In addition, all samples did not reach the plateau region at $p/p_0 \approx 1$ where p_o is the saturation vapor pressure and p the partial pressure at a certain gas volume, implying that large amount of macropores was contained in the structure of PBZ-based organic xerogels.
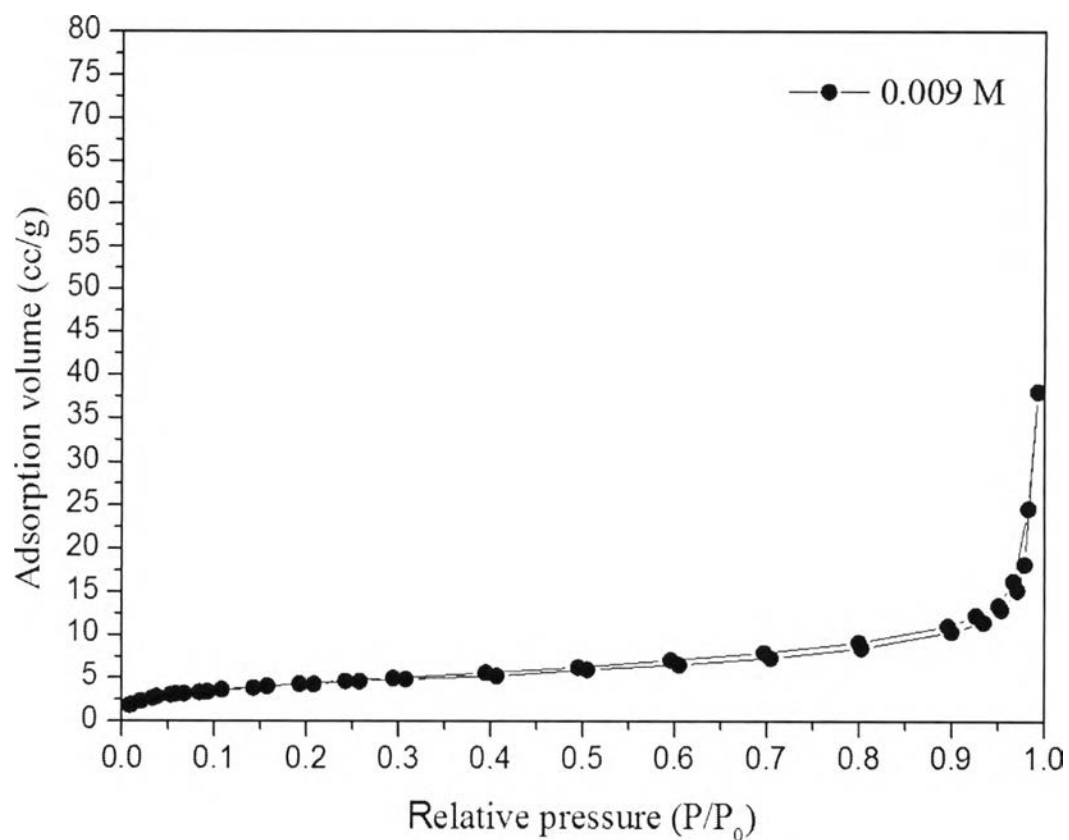
The mesopore and macropore size distribution of all samples, calculated by BJH method, was illustrated in Figure 4.9, 4.11, 4.13, and 4.15. All samples are showed the higher amount of macropore volume and average mesopore size about 0.08-0.11 cc/g and 3.59-4.58 nm, respectively. Moreover, amount of mesopore volume of carbon xerogels derived from Poly(ethylene glycol)-*block*-poly(propylene glycol)-*block*-poly(ethylene glycol) at concentration of 0.003-0.090 M was obviously increased. According to the microporous property of the obtained carbon xerogels, micropore size distributions, calculated by BJH method. All samples showed the very small amount of micropore and average mesopore size about 0.01 cc/g and 0.37-1.00 nm.
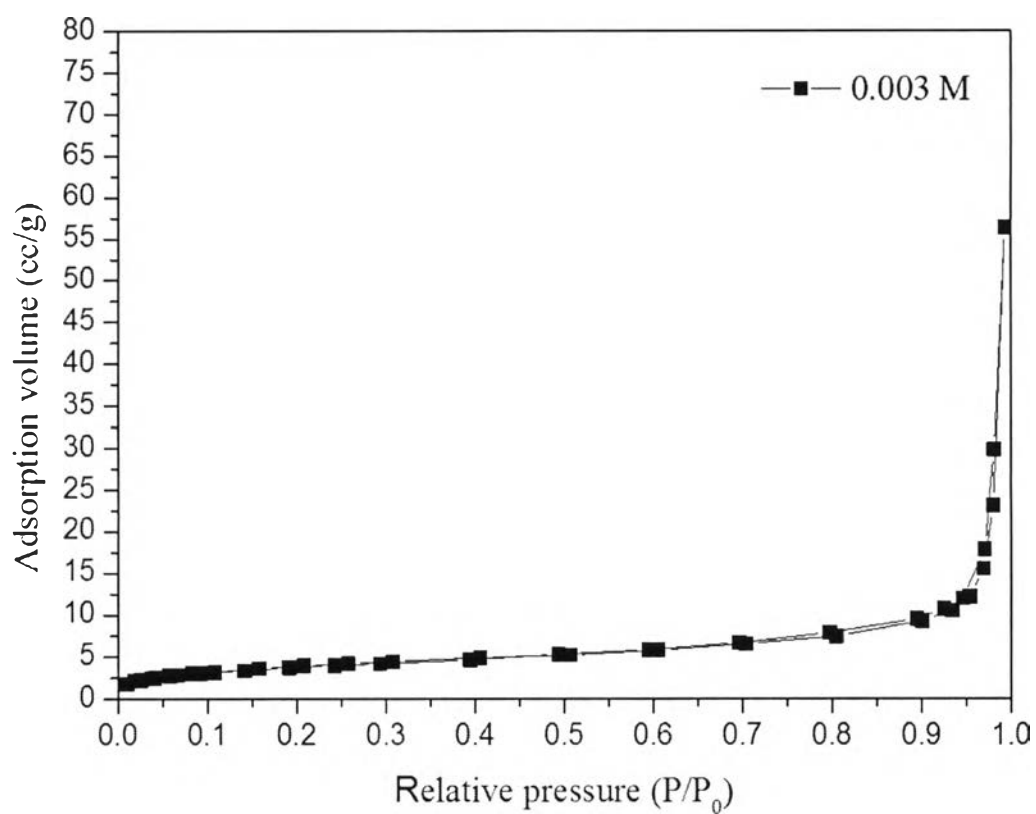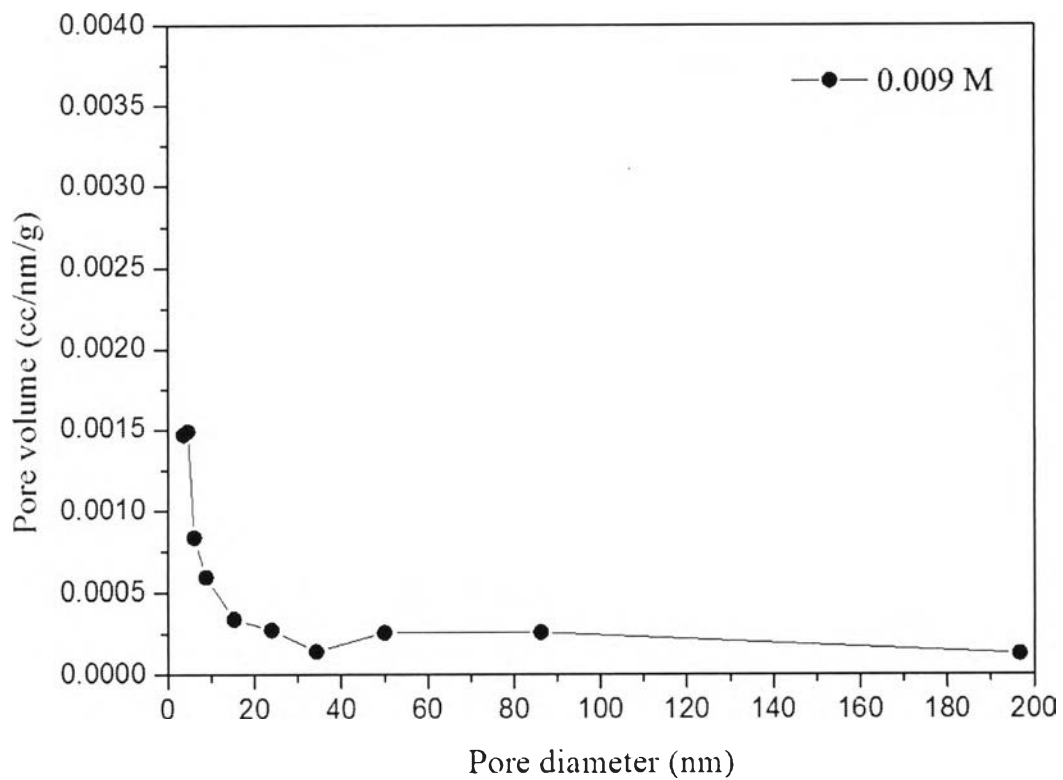
Figure 4.8 N_2 adsorption-desorption isotherms of polybenzoxazine-based organic xerogels using 0.003 M of Poly(ethylene glycol)-*block*-poly(propylene glycol)-*block*-poly(ethylene glycol).
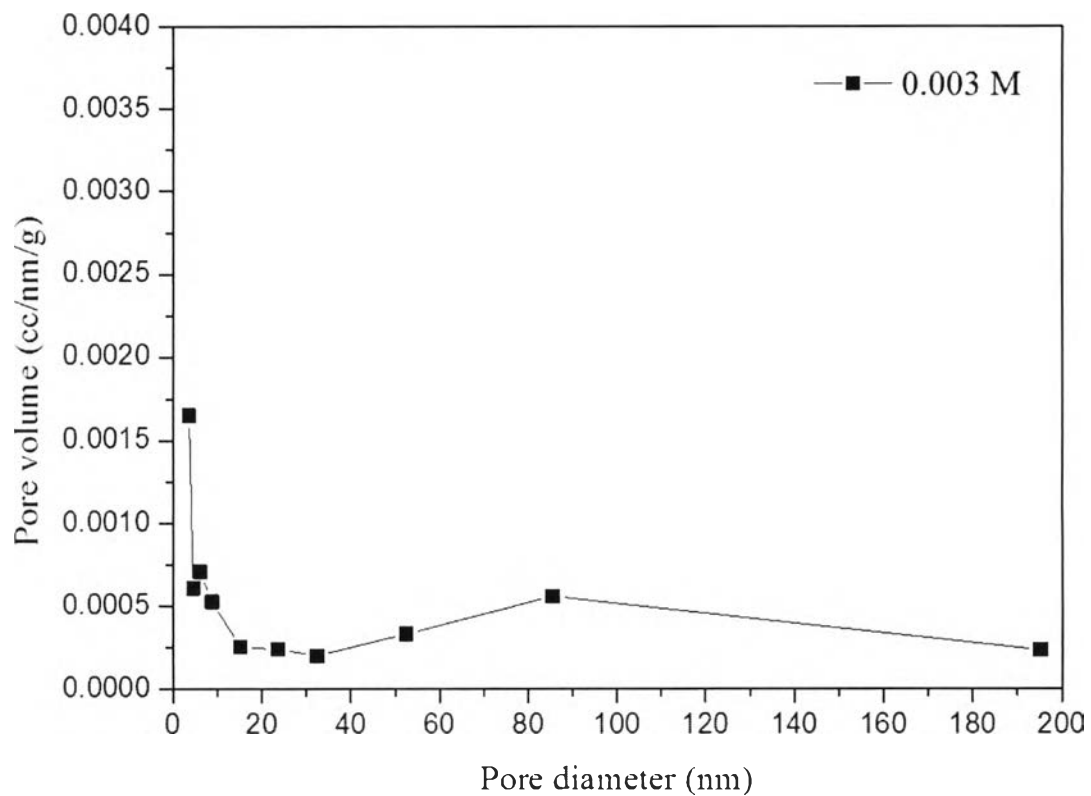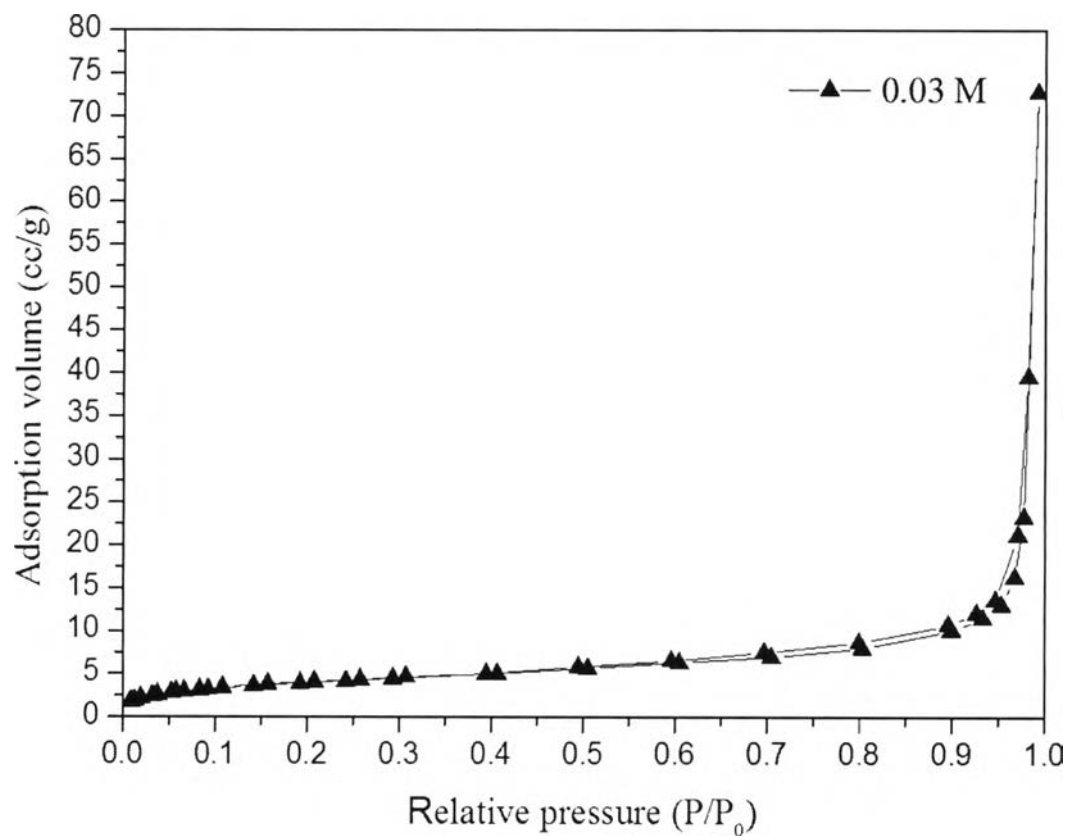
Figure 4.9 Mesopore size distributions of polybenzoxazine-based organic xerogels using 0.003 M of Poly(ethylene glycol)-*block*-poly(propylene glycol)-*block*-poly(ethylene glycol), determined by BJH method.
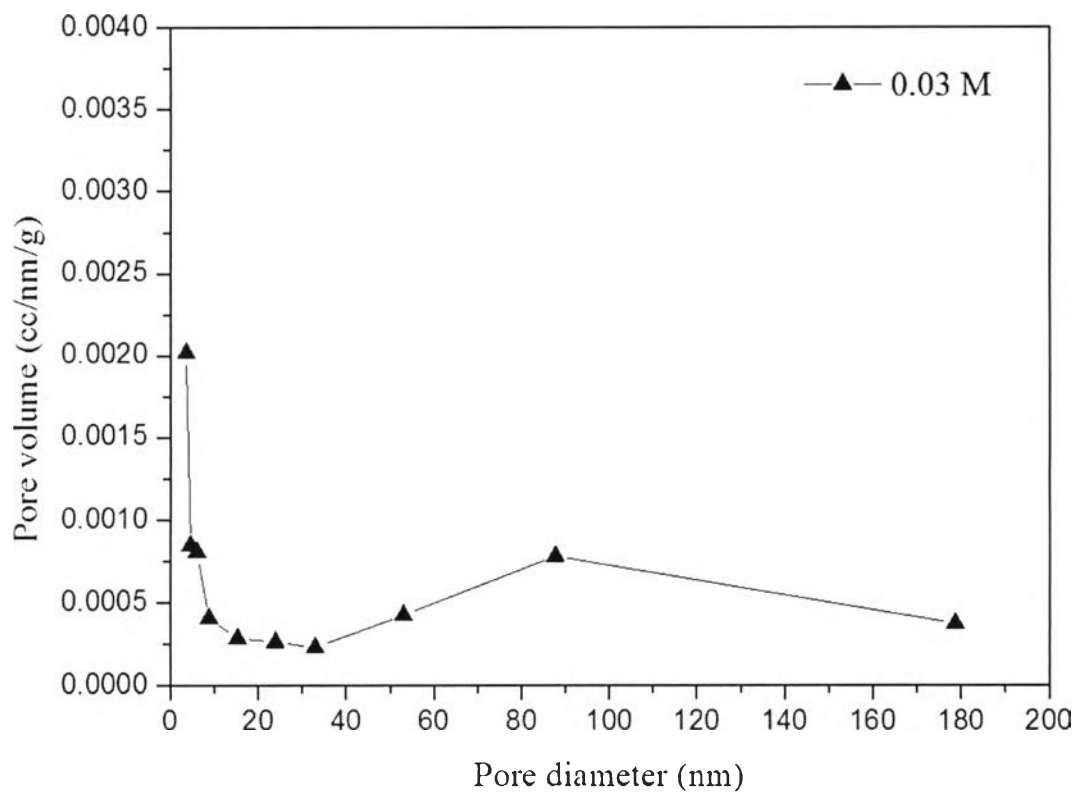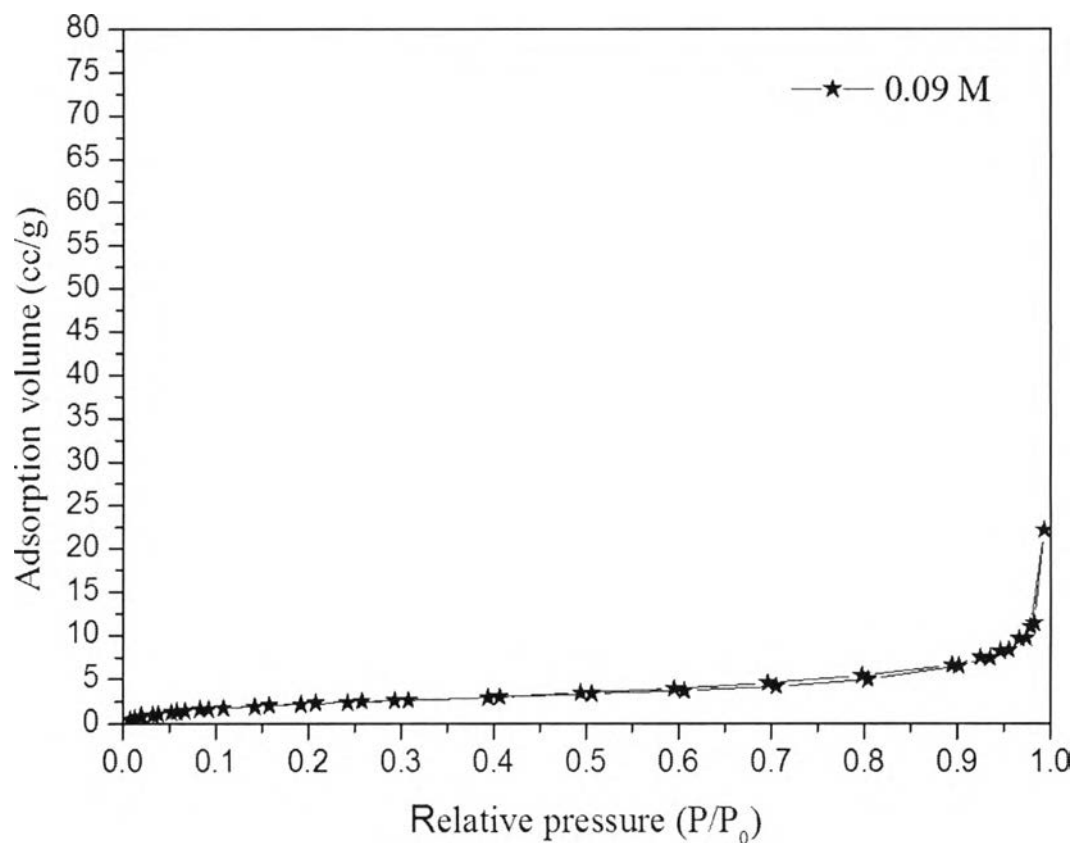
Figure 4.10 N_2 adsorption-desorption isotherms of polybenzoxazine-based organic xerogels using 0.009 M of Poly(ethylene glycol)-*block*-poly(propylene glycol)-*block*-poly(ethylene glycol).

Figure 4.11 Mesopore size distributions of polybenzoxazine-based organic xerogels using 0.009 M of Poly(ethylene glycol)-*block*-poly(propylene glycol)-*block*-poly(ethylene glycol), determined by BJH method.

Figure 4.12 N_2 adsorption-desorption isotherms of polybenzoxazine-based organic xerogels using 0.03 M of Poly(ethylene glycol)-*block*-poly(propylene glycol)-*block*-poly(ethylene glycol).
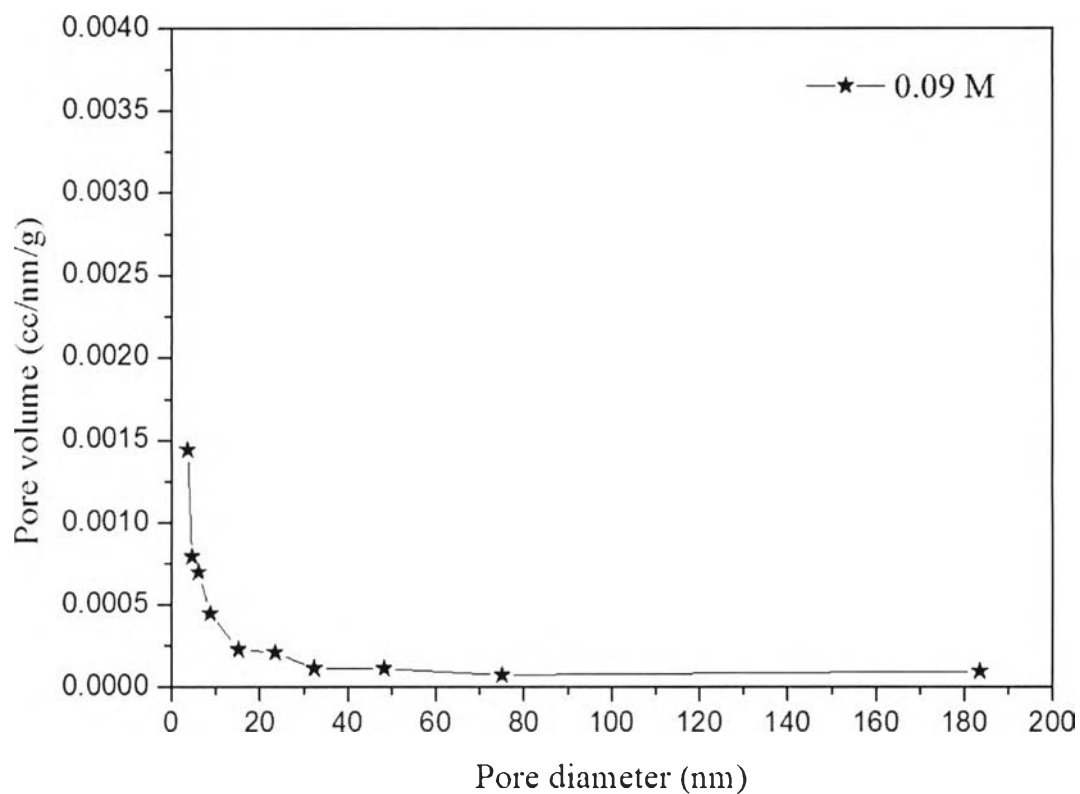
Figure 4.13 Mesopore size distributions of polybenzoxazine-based organic xerogels using 0.03 M of Poly(ethylene glycol)-*block*-poly(propylene glycol)-*block*-poly(ethylene glycol), determined by BJH method.

Figure 4.14 N$_2$ adsorption-desorption isotherms of polybenzoxazine-based organic xerogels using 0.09 M of Poly(ethylene glycol)-*block*-poly(propylene glycol)-*block*-poly(ethylene glycol).

Figure 4.15 Mesopore size distributions of polybenzoxazine-based organic xerogels using 0.09 M of Poly(ethylene glycol)-*block*-poly(propylene glycol)-*block*-poly(ethylene glycol), determined by BJH method.

Table 4.2 Pore characteristics of organic xerogels by ambient pressure drying at different concentrations of Poly(ethylene glycol)-*block*-poly(propylene glycol)-*block*-poly(ethylene glycol) surfactant.

Sample	S_{BET} (m^2/g)	V_{micro} (cm^3/g)	V_{meso} (cm^3/g)	V_{macro} (cm^3/g)	V_{total} (cm^3/g)	APD_{micro} (nm)	APD_{meso} (nm)
0.003	14	0.01	0.08	0.06	0.15	0.37	3.59
0.009	15	0.01	0.05	0.17	0.23	0.37	4.58
0.030	15	0.01	0.11	0.20	0.32	0.50	3.59
0.090	19	0	0.03	0.32	0.35	1.00	3.59

Note : S_{BET} : BET surface area ; S_{micro} : micropore surface area ; V_{micro} : micropore volume ; V_{meso} : mesopore volume ; V_{macro} : macropore volume ; V_{total} : total pore volume ; APD_{micro} : average micropore diameter ; APD_{meso} : average mesopore diameter